

AperTO - Archivio Istituzionale Open Access dell'Università di Torino

**Chemoselective hydrogenation of halonitroaromatics over gamma-Fe<sub>2</sub>O<sub>3</sub>-supported platinum nanoparticles: The role of the support on their catalytic activity and selectivity**

**This is the author's manuscript**

*Original Citation:*

*Availability:*

This version is available <http://hdl.handle.net/2318/140589> since 2017-06-28T14:31:44Z

*Published version:*

DOI:10.1016/j.molcata.2012.10.007

*Terms of use:*

Open Access

Anyone can freely access the full text of works made available as "Open Access". Works made available under a Creative Commons license can be used according to the terms and conditions of said license. Use of all other works requires consent of the right holder (author or publisher) if not exempted from copyright protection by the applicable law.

(Article begins on next page)

This Accepted Author Manuscript (AAM) is copyrighted and published by Elsevier. It is posted here by agreement between Elsevier and the University of Turin. Changes resulting from the publishing process - such as editing, corrections, structural formatting, and other quality control mechanisms - may not be reflected in this version of the text. The definitive version of the text was subsequently published in JOURNAL OF MOLECULAR CATALYSIS. A: CHEMICAL, 366, 2013, 10.1016/j.molcata.2012.10.007.

You may download, copy and otherwise use the AAM for non-commercial purposes provided that your license is limited by the following restrictions:

- (1) You may use this AAM for non-commercial purposes only under the terms of the CC-BY-NC-ND license.
- (2) The integrity of the work and identification of the author, copyright owner, and publisher must be preserved in any copy.
- (3) You must attribute this AAM in the following format: Creative Commons BY-NC-ND license (<http://creativecommons.org/licenses/by-nc-nd/4.0/deed.en>), 10.1016/j.molcata.2012.10.007

The publisher's version is available at:

<http://linkinghub.elsevier.com/retrieve/pii/S138111691200338X>

When citing, please refer to the published version.

Link to this full text:

<http://hdl.handle.net/2318/140589>

# Chemoselective hydrogenation of halonitroaromatics over $\gamma$ -Fe<sub>2</sub>O<sub>3</sub>-supported platinum nanoparticles: The role of the support on their catalytic activity and selectivity

Claudio Evangelisti<sup>a</sup>

Laura Antonella Aronica<sup>b</sup>

Gianmario Martra<sup>c</sup>

Chiara Battocchio<sup>d</sup>

Giovanni Polzonetti<sup>d</sup>

a

CNR, Institute of Molecular Science and Technologies (CNR-ISTM), Via G. Fantoli 16/15, 20138 Milano, Italy

b

Department of Chemistry and Industrial Chemistry, Via Risorgimento 35, 56126 Pisa, Italy

c

Department of Chemistry IFM & NIS Interdepartmental Centre of Excellence, Via P. Giuria 7, 10125 Torino, Italy

d

Department of Physics, INSTM e CISDiC, University of Roma Tre, Via della Vasca Navale 84, 00146 Roma, Italy

## Abstract

Solvated platinum atoms, obtained by metal vapour synthesis (MVS), were conveniently used to prepare  $\gamma$ -iron oxide and  $\gamma$ -alumina supported Pt catalysts containing small metal nanoparticles of controlled size, ranging 0.5–3.0 nm in diameter (HR-TEM). The  $\gamma$ -Fe<sub>2</sub>O<sub>3</sub>-supported Pt system showed higher catalytic activity and selectivity than those of a similarly prepared  $\gamma$ -Al<sub>2</sub>O<sub>3</sub>-supported system in the selective hydrogenation reactions of p- and o-chloronitrobenzene to the corresponding haloanilines, in mild reaction conditions (25 °C, 0.1 MPa hydrogen pressure) (p-chloronitrobenzene: specific activity (SA) = 59.5 min<sup>-1</sup>, Selectivity (Sel.) = 99.9%; o-chloronitrobenzene: SA = 42.8 min<sup>-1</sup>, Sel. = 99.2%). The Pt/ $\gamma$ -Fe<sub>2</sub>O<sub>3</sub> system also showed high catalytic efficiency (Sel. > 98%, at 100% of conversion) in the selective hydrogenations of m-chloro-, p- and o-bromo- and p- and o-iodonitrobenzenes. XPS structural studies performed on a pristine Pt/ $\gamma$ -Fe<sub>2</sub>O<sub>3</sub> sample as well as on a sample recovered after the reaction, indicate that the catalytic process did not induce permanent modification in the chemical and/or electronic structure of the catalyst according with the high reusability of the system.

## Keywords

Platinum catalyst, Iron oxide, Hydrogenation, Halonitrobenzenes, Metal vapour synthesis

## 1. Introduction

Aromatic haloamine derivatives are valuable intermediates in the synthesis of pharmaceuticals, agrochemicals, perfumes and dyes [1,2]. The catalytic hydrogenation of aromatic nitro-compounds over supported metal catalysts provides a clean route to the corresponding aromatic amines, with lower economical and environmental impact than alternatives non-catalytic processes [3,4]. Nevertheless, the catalytic reduction of halogen-substituted nitroaromatic compounds is often problematic because of the extensive hydrogenolysis of carbon–halogen bond which affords a mixture of haloaniline and de-halogenated aniline products [5]. De-halogenation reactions have been reported to occur also with palladium [6], platinum [7], rhodium [8], nickel [9] and copper chromite [10]. Recently, the application of new supported metals, such as Au [11,12] or Ag [13], which showed high selectivity but low catalytic activity, were proposed and developed. Despite that, Pt-based catalysts continue to receive a particular attention due to their fast reaction rate and low yield of de-halogenation products (<20%) [14]. Their performances were shown to be strongly related to different parameters including reaction conditions (temperature, pressure, stirring rate, ...) [15], the presence of specific promoters or additives [16], the platinum particle size distribution [3,17] or the kind of catalyst support [18–20]. Among them metal/support interaction can have a great influence on the electronic density of metal particles by charge transfer or polarization by partially reducible supports, generating special active sites at the metal–support boundary regions. Recently, it has been reported that a Pt–iron oxide nanocomposite, prepared by co-precipitation of iron hydroxide colloid and Pt colloid in ethylene glycol, exhibits high selectivity (>99%) in the hydrogenation of o-chloronitrobenzene and bromonitrobenzenes [21,22].

In order to get a deeper insight into the role of the support and the influence of the preparative route on the catalytic activity and selectivity of the catalyst we report here the preparation of new Pt system, obtained following the metal vapour synthesis (MVS) procedure [23–25], containing small Pt nanoparticles deposited on commercially available  $\gamma$ -Fe<sub>2</sub>O<sub>3</sub> support.

The catalytic activity and selectivity of the Pt/ $\gamma$ -Fe<sub>2</sub>O<sub>3</sub> in p- and o-chlorobenzene hydrogenations, performed in mild reaction conditions (298 K, 0.1 MPa H<sub>2</sub>), were compared with that of a similarly prepared Pt/ $\gamma$ -Al<sub>2</sub>O<sub>3</sub> system, which was previously demonstrated as a valuable catalyst in this reaction [26], as well as a commercial Pt/ $\gamma$ -Al<sub>2</sub>O<sub>3</sub> catalyst. The high catalytic efficiency of the  $\gamma$ -Fe<sub>2</sub>O<sub>3</sub>-supported system was confirmed in the selective hydrogenation of bromo- and iodonitrobenzene derivatives. The structural features of the  $\gamma$ -Fe<sub>2</sub>O<sub>3</sub> and  $\gamma$ -Al<sub>2</sub>O<sub>3</sub>-supported systems were investigated by transmission

electron microscopy (TEM) analyses. Moreover, in order to obtain more information on the electronic and chemical properties of the Pt/ $\gamma$ -Fe<sub>2</sub>O<sub>3</sub> system, X-ray photoelectron spectroscopy (XPS) studies on a pristine sample and on a recovered sample after a catalytic test, were performed.

## 2. Experimental

### 2.1. Materials and apparatus

All operations involving the MVS products were performed under a dry argon atmosphere. Mesitylene was purified by conventional methods, distilled and stored under argon. 1,3-divinyl-1,1,3,3-tetramethyldisiloxane (DVS), 1-chloro-4-nitrobenzene, 1-chloro-2-nitrobenzene, 1-chloro-3-nitrobenzene, 1-bromo-4-nitrobenzene, 1-bromo-2-nitrobenzene, 1-iodo-2-nitrobenzene were supplied from Aldrich and used as received. Commercial  $\gamma$ -Al<sub>2</sub>O<sub>3</sub> (Chimet product, type 49, surface area 110 m<sup>2</sup>/g, mean particle diameter 31  $\mu$ m),  $\gamma$ -Fe<sub>2</sub>O<sub>3</sub> powder (Aldrich products, surface area 50–245 m<sup>2</sup>/g, particles < 50 nm) was dried in a static oven before use.

Commercial platinum on  $\gamma$ -Al<sub>2</sub>O<sub>3</sub> (1 wt.% of Pt, surface area 250 m<sup>2</sup>/g) was an Aldrich product.

The amount of platinum in the solvated Pt atoms solutions was determined by Inductively Coupled Plasma-Optical Emission Spectrometers (ICP-OES) with a Spectro-Genesis instrument, with a software Smart Analyzer Vision. The metal-containing mesitylene solution (1 mL) was heated over a heating plate in a porcelain crucible, in the presence of aqua regia (2 mL), six times. The solid residue was dissolved in 0.5 M aqueous HCl, and the solution was analyzed by ICP-OES spectrometer.

The GLC analyses were performed on a Perkin-Elmer Auto System gas chromatograph, equipped with a flame ionization detector (FID), using a SiO<sub>2</sub> column (BP-1, 12 m  $\times$  0.3 mm, 0.25  $\mu$ m) and helium as carrier gas.

High resolution transmission electron microscopy (HR-TEM) images of the materials were obtained using a JEOL 3010-UHR with an acceleration potential of 300 kV. To obtain a good dispersion and avoid any contamination, lacey carbon Cu grids were briefly contacted with the powders, resulting in the adhesion of some particles to the sample holders by electrostatic interactions.

Histograms of the particle size distribution were obtained by considering at least 500 particles on the TEM images, and the mean particle diameter ( $d_m$ ) was calculated as  $d_m = \sum d_i n_i / \sum n_i$ , where  $n_i$  was the number of particles of diameter  $d_i$ . The counting was carried out on electron micrographs obtained starting from 300,000 magnification, where Pd particles well contrasted with respect to the support were clearly detected. The graduation of the particle size scale was 0.5 nm.

XPS analysis was performed in an instrument of our own design and construction, consisting of a preparation and an analysis UHV chamber, equipped with a 150 mm mean radius hemispherical electron analyser with a four-elements lens system with a 16-channel detector giving a total instrumental resolution of 1.0 eV as measured at the Ag 3d<sub>5/2</sub> core level. Mg K $\alpha$  non-monochromatised X-ray radiation ( $h\nu = 1253.6$  eV) was used for acquiring core level spectra of all samples (C1s, Pt4f, O1s and Fe2p). The spectra were energy referenced to the C1s signal of aliphatic C atoms having a binding energy BE = 285.00 eV, due to surface contamination, as expected for XPS measurements performed on solid samples exposed to air. Atomic ratios were calculated from peak intensities by using Scofield's cross-section values and calculated  $\lambda$  factors [27]. Curve-fitting analysis of the C1s, Pt4f, O1s and Fe2p spectra was performed using Voigt profiles as fitting functions, after subtraction of a Shirley-type background [28].

### 2.2. Preparation of platinum catalysts

According to a previously reported preparation [25], Pt vapour generated at 10–2 Pa by resistive heating of a tungsten wire surface coated with electrodeposited platinum (105 mg), was co-condensed at liquid

nitrogen temperature with mesitylene (60 mL) in a glass reactor described elsewhere [23,24]. The reactor chamber was heated to the melting point of the solid matrix ( $-40\text{ }^{\circ}\text{C}$ ), and the resulting yellow-brown solution (55 mL) was worked up under argon atmosphere with the use of the standard Schlenk technique and kept at low temperature ( $-30/-40\text{ }^{\circ}\text{C}$ ). The platinum content of the mesitylene solvated platinum solution, measured by ICP-OES, was 1.6 mg/mL. 10 mL of DVS were added to the Pt/mesitylene solution and the resulting thermally stable solution was stirred at  $25\text{ }^{\circ}\text{C}$  for 15 min. The DVS-stabilized Pt/mesitylene solution (7.4 mL, 10 mg Pt) was added to a dispersion of  $\gamma\text{-Al}_2\text{O}_3$  and  $\gamma\text{-Fe}_2\text{O}_3$  (1 g), respectively, in mesitylene (20 mL). The mixture was stirred for 12 h at room temperature. The colourless mesitylene was removed and the light-brown solid, containing 1 wt.% Pt, was washed with n-pentane and dried under reduced pressure.

### 2.3. Catalytic hydrogenations

Hydrogenation of halonitrobenzene was carried out in a 50-mL round-bottomed flask fitted with a magnetic stirring bar (stirring rate = 1250 rpm) and under atmospheric hydrogen pressure (0.1 MPa) at  $25\text{ }^{\circ}\text{C}$ . Prior to the reaction, 20 mg of Pt catalyst (containing 1 wt.% Pt, 0.001 mmol) was activated under hydrogen for 15 min, then 2.56 mmol of halonitrobenzene (404 mg for 1-chloro-4-nitrobenzene, 1-chloro-2-nitrobenzene and 1-chloro-3-nitrobenzene; 517 mg for 1-bromo-4-nitrobenzene and 1-bromo-2-nitrobenzene; 637 mg for 1-iodo-2-nitrobenzene and 1-iodo-4-nitrobenzene) in 10 mL of methanol was added to the reaction system to start the reaction.

Reactants and products are identified by comparison of their GLC retention times with those of authentic samples. The semi-quantitative analysis of trace aniline (AN) in the reaction mixture was conducted by comparing the AN peak area in GC with those of standard solutions with ratios of AN to haloaniline (XAN) less than 0.1%. Where reported the Pt/ $\gamma\text{-Fe}_2\text{O}_3$  system was magnetically separated from the reaction mixture at the bottom of round-bottomed flask, washed with methanol, and further reused by adding a new amount of halonitrobenzene substrate and methanol as solvent.

### 3. Results and discussion

It has been recently reported that the addition of 1,3-divinyl-1,1,3,3-tetramethyldisiloxane (DVS) ligand to mesitylene solvated Pt atoms, obtained by MVS, is a suitable way to quench the growth processes of Pt particle in solution making them stable at  $25\text{ }^{\circ}\text{C}$  and valuable starting materials for the deposition of Pt nanoparticles of controlled size on solid supports [25]. Following that procedure, nanostructured Pt systems deposited on  $\gamma\text{-Al}_2\text{O}_3$  and  $\gamma\text{-Fe}_2\text{O}_3$ , respectively, containing 1 wt.% of Pt, were prepared.

Representative TEM images of the Pt/ $\gamma\text{-Al}_2\text{O}_3$  and Pt/ $\gamma\text{-Fe}_2\text{O}_3$  systems are given in Fig. 1. For obtained samples a statistical evaluation of the Pt particles size was carried out. In the case of Pt/ $\gamma\text{-Al}_2\text{O}_3$  (Fig. 1, section A) a large part of the particles were monitored in the interval of 0.8–3.0 nm with a more abundant population around 2 nm ( $d_m = 1.9 \pm 1.2\text{ nm}$ ). The Pt particles resulted well separated, but located very close to each other. As concerns Pt/ $\gamma\text{-Fe}_2\text{O}_3$  the obtained particle size distribution was very narrow as well (0.8–3.3 nm) (Fig. 1, section B) and small Pt particles were well separated and well dispersed on the support surface with a more abundant population also around 2 nm ( $\pm 1.2$ ). It is necessary to take into the consideration that the detection limit of the TEM technique is around 1 nm and the aggregation phenomena of sub-nanometric metal particles under the electron beam during HR-TEM observation cannot be excluded as well. As a consequence the real mean size of MVS Pt particles could be even smaller.

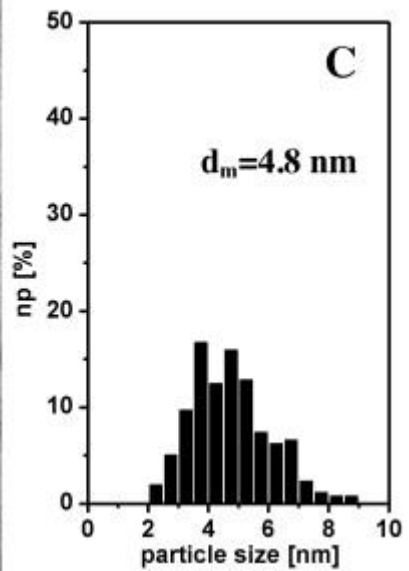
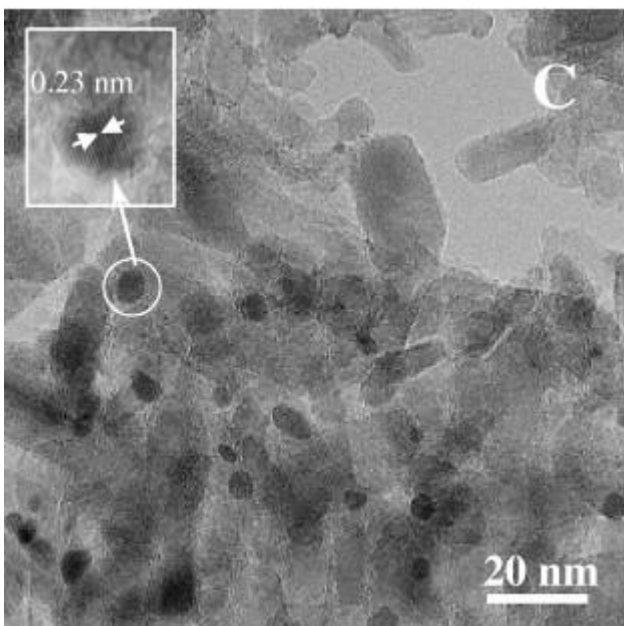
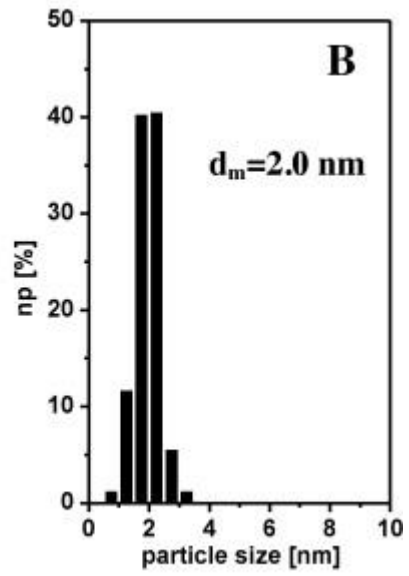
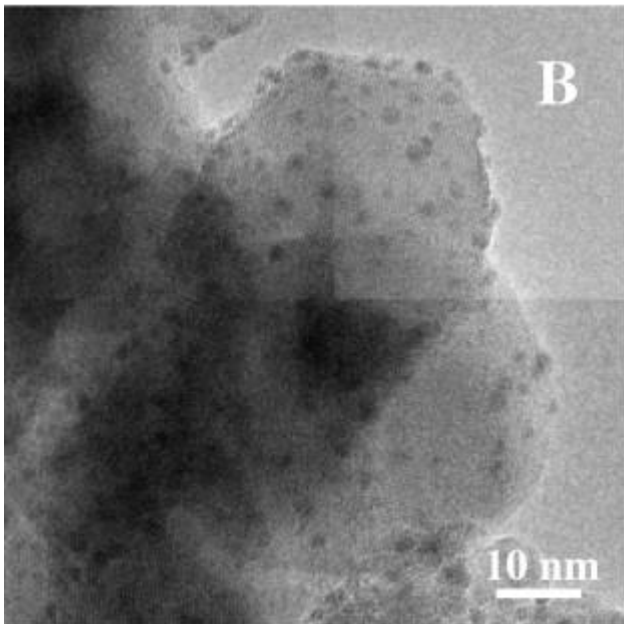
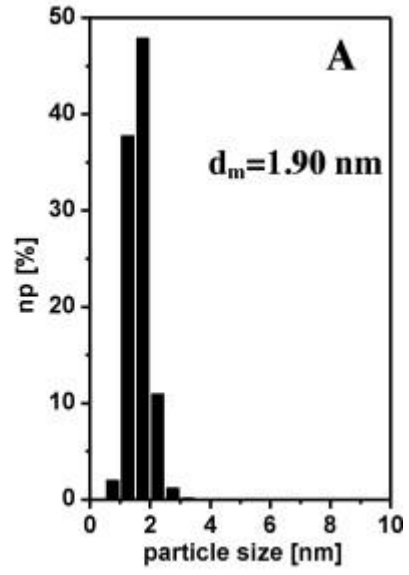
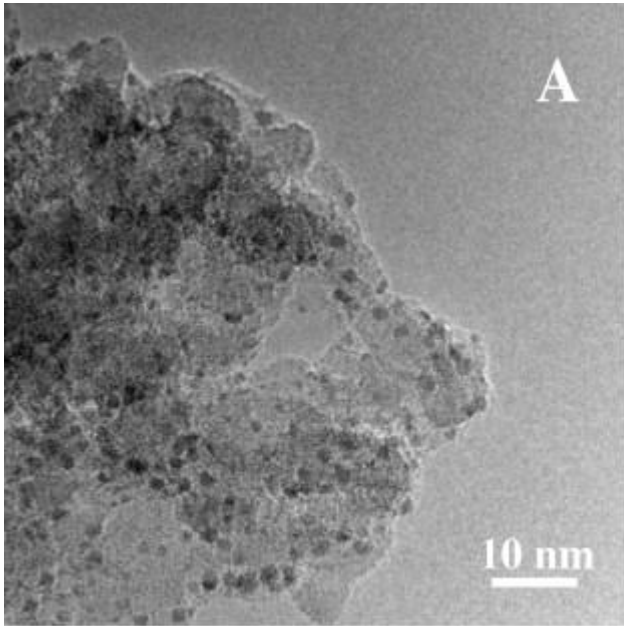


Fig. 1. TEM images and histograms of the particle size distributions obtained for MVS-derived Pt/ $\gamma$ -Al<sub>2</sub>O<sub>3</sub> (section A), Pt/ $\gamma$ -Fe<sub>2</sub>O<sub>3</sub> (section B) and Pt/ $\gamma$ -Al<sub>2</sub>O<sub>3</sub> commercial sample (section C), original magnification: 30,000 $\times$ .

On the other hand, the commercial Pt/ $\gamma$ -Al<sub>2</sub>O<sub>3</sub> sample showed broader particle size distribution (2.0–9.0 nm) with a mean diameter at 4.8 nm ( $\pm$ 3.0).

In Pt/ $\gamma$ -Al<sub>2</sub>O<sub>3</sub> and Pt/ $\gamma$ -Fe<sub>2</sub>O<sub>3</sub> catalysts (sections A and B of Fig. 1, respectively), the size of the metal particles was so small to prevent the attainment at high magnification of a contrast high enough to allow a clear observation of lattice fringes. Conversely, in the case of the commercial Pt- $\gamma$ -Al<sub>2</sub>O<sub>3</sub> catalyst (C), which exhibited larger metal particles, in some cases lattice fringes 0.23 nm apart, corresponding to the (1 1 1) interplanar distance for Pt crystals with fcc structure (File ASTM 4-0802).

X-ray photoelectron spectroscopy (XPS) results obtained from studies on the Pt/ $\gamma$ -Fe<sub>2</sub>O<sub>3</sub> pristine system are collected and compared in Fig. 2 and in Table 1.

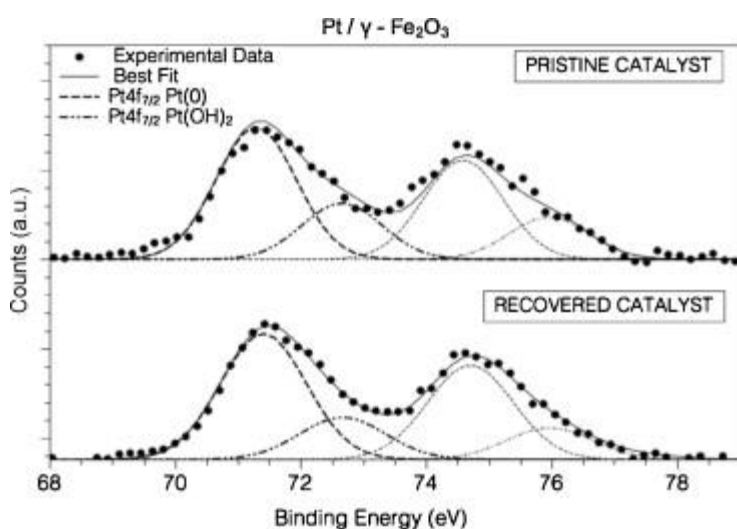


Fig. 2. Pt4f spectra of MVS-derived Pt/ $\gamma$ -Fe<sub>2</sub>O<sub>3</sub> system pristine and recovered after the catalytic process.

Table 1. BE, FWHM, qualitative and semi-quantitative analysis of Pt/ $\gamma$ -Fe<sub>2</sub>O<sub>3</sub> system pristine and recovered after the catalytic process.

	Signal	BE (eV)	FWHM (eV)	Group/chemical specie	Atomic ratio Pti/Pttot
Pt/ $\gamma$ -Fe <sub>2</sub> O <sub>3</sub> (pristine)	C1s	285.00	1.84	C—C	
		529.80	1.64	Fe <sub>2</sub> O <sub>3</sub>	
	O1s	532.22	1.64	OH	
		533.49	1.64	H <sub>2</sub> O	
Pt4f7/2		71.29	1.85	Pt(0)	0.84
		72.66	1.85	Pt(OH) <sub>2</sub>	0.16
	Fe2p3/2	711.60	4.99	Fe <sub>2</sub> O <sub>3</sub>	
Pt/ $\gamma$ -Fe <sub>2</sub> O <sub>3</sub> (recovered)	C1s	285.00	1.89	C—C	



Signal	BE (eV)	FWHM (eV)	Group/chemical specie	Atomic ratio Pti/Pttot
	530.28	1.75	Fe2O3 + PtO	
O1s	531.99	1.75	OH	
	533.49	1.75	H2O	
Pt4f7/2	71.41	1.61	Pt(0)	0.72
	72.67	1.61	Pt(OH)2	0.28
Fe2p3/2	711.36	4.25	Fe2O3	

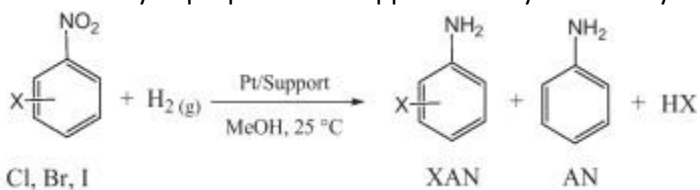
The core level binding energy (BE), the full width at half-maxima (FWHM) and atomic ratio  $N(\text{Pti})/N(\text{Pttot})$  values were analyzed with particular attention to the Pt4f signal components, which are of major interest for the study of the nanostructured catalyst, and for the assessment of the Pt/Fe2O3 interaction. Pt4f is usually used as reference signal for the XPS study of Pt atoms, since it has the highest photoemission cross-section among other Pt signals (i.e., the highest signal intensity) [29,30].

The Pt4f spectrum of the system is reported at the top of Fig. 2; by means of a curve-fitting analysis, each Pt4f spin-orbit component of the experimental spectrum results from the combination of two peaks as associated to two platinum atoms involved in different chemical environments. The main Pt4f7/2 peak is found at 71.40 eV BE and has been attributed to metallic platinum (Pt(0)) interacting with  $\gamma$ -Fe2O3 oxide. In fact, the Pt4f7/2 BE value expected for bulk Pt metal on the basis of previous measurements and in agreement with literature reports is 71.00 eV; as extensively discussed in [21], the BE positive shift of about 0.4 eV observed in the Pt-supported catalysts indicates that an electron transfer occurs from the Pt particles to the iron oxide supports, leading to Pt nanoparticles of an electron-deficient state in the heterogeneous catalysts. The pair of spin-orbit components found at higher BE values (Pt4f7/2 BE = 72.66 eV) is related to oxidized Pt atoms, and, as suggested by literature data, is indicative of Pt(OH)2 species at least on the nanoparticles surface [31]. The semi-quantitative analysis indicates that Pt(OH)2 species are nearly 16% of the total Pt amount.

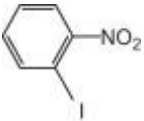
As reported in Table 1, the measured XPS Fe2p signal shows a single spin-orbit pair with the main Fe2p3/2 component at 711.60 eV BE, as expected for Fe2O3; iron oxide stoichiometry is also confirmed by the estimated Fe/Ooxide atomic ratio of about 2/3. The O1s spectrum appears structured, and three main spectral components can be detected by curve fitting [32]. The main contribution at about 530 eV is related to iron oxide; the small peak at about 532 eV is attributed to OH groups bonded to metals (Pt(OH)2) as well as to OH groups of surface contaminants adsorbed on the sample surface, as expected for XPS measurements performed on solid samples exposed to air; the third component at nearly 534 eV BE arises by physisorbed H2O molecules. In conclusion, XPS analysis results indicate that a weak interaction occurs between Pt atoms and  $\gamma$ -Fe2O3 support, resulting in an electron-deficient state of the Pt nanoparticles in the catalyst, due to an electron transfer from Pt atoms to the iron oxide.

The results obtained in the hydrogenation of halonitrobenzene compounds over the Pt/ $\gamma$ -Fe2O3 system compared with the analogous  $\gamma$ -Al2O3-supported system and a commercial Pt/ $\gamma$ -Al2O3 catalyst are summarized in Table 2. The reactions were performed under mild reaction conditions (25 °C, 0.1 MPa hydrogen pressure) using a molar ratio substrate/Pt = 2560.

Table 2. Catalytic properties of supported Pt systems in hydrogenation of halonitrobenzenes.



Run	Substrate	Catalyst	Reaction time <sup>a</sup> (min)	Specific activity (SA) <sup>b</sup> (min <sup>-1</sup> )	Selectivity (%)	
					XAN	AN
1		Pt/ $\gamma$ -Fe <sub>2</sub> O <sub>3</sub>	48	59.5	99.9	0
2		Pt/ $\gamma$ -Al <sub>2</sub> O <sub>3</sub>	60	44.2	96.2	3.8
3		Pt/ $\gamma$ -Al <sub>2</sub> O <sub>3</sub> commercial	330	8.7	97.3	2.7
4		Pt/ $\gamma$ -Fe <sub>2</sub> O <sub>3</sub>	60	42.8	99.2	0.8
5		Pt/ $\gamma$ -Al <sub>2</sub> O <sub>3</sub>	126	29.8	93.4	6.6
6		Pt/ $\gamma$ -Al <sub>2</sub> O <sub>3</sub> commercial	510	5.1	96.0	4.0
7		Pt/ $\gamma$ -Fe <sub>2</sub> O <sub>3</sub>	72	39.2	99.5	0.5
8		Pt/ $\gamma$ -Fe <sub>2</sub> O <sub>3</sub>	35	85.3	99.2	0.8
9		Pt/ $\gamma$ -Fe <sub>2</sub> O <sub>3</sub>	45	64.2	98.6	1.4
10		Pt/ $\gamma$ -Fe <sub>2</sub> O <sub>3</sub>	320	8.25	98.8	1.2

Run	Substrate	Catalyst	Reaction time <sup>a</sup> (min)	Specific activity (SA) <sup>b</sup> (min <sup>-1</sup> )	Selectivity (%)	
					XAN	AN
11		Pt/ $\gamma$ -Fe <sub>2</sub> O <sub>3</sub>	380	6.6	98.0	2.0

Reaction conditions: solvent = MeOH (10 mL), temperature = 25 °C, 20 mg of Pt catalyst (containing 1 wt.% Pt),  $1 \times 10^{-3}$  mmol), 2.56 mmol of halonitrobenzene.

a

Time at 100% conversion of halonitrobenzene.

b

Specific activity is calculated as (mol converted substrate)/(mol Pt  $\times$  min)) at about 50% of conversion.

The MVS-derived Pt/ $\gamma$ -Fe<sub>2</sub>O<sub>3</sub> and Pt/ $\gamma$ -Al<sub>2</sub>O<sub>3</sub> systems showed considerably higher catalytic activity than commercial Pt/ $\gamma$ -Al<sub>2</sub>O<sub>3</sub>, having the same metal loading, in the hydrogenation of p- and o-chloronitrobenzene (runs 1–6). The differences in catalytic activity can be strictly related to the higher platinum surface area of MVS-derived samples as evidenced from the particle size distributions obtained from TEM analyses (Fig. 1).

The Pt/ $\gamma$ -Fe<sub>2</sub>O<sub>3</sub> system showed the highest catalytic activity of the examined systems and comparable with other reported Pt–iron oxide systems [21] in hydrogenation of p- and o-chloronitrobenzene (SA = 59.5 min<sup>-1</sup>, run 1, and SA = 42.8 min<sup>-1</sup>, run 4, respectively). This system showed also higher selectivity than both  $\gamma$ -Al<sub>2</sub>O<sub>3</sub>-supported systems leading top-chloroaniline as unique product (>99.9%, run 1) in the hydrogenation of the corresponding nitro-compound and a very high selectivity (99.2%, run 4) to o-chloroaniline in the hydrogenation reaction of o-chloronitrobenzene. In any cases, as easily predictable, the increase of steric hindrance (from p- to o-) determines a slight decrease of reaction rate which in turn could be the cause of a small decrease of selectivity [2,14].

The MVS-derived Pt/ $\gamma$ -Al<sub>2</sub>O<sub>3</sub> system, whose containing Pt particle sizes was significantly smaller than those of the commercial sample (see HR-TEM analyses), showed slightly lower selectivity both in p-chloronitrobenzene (96.2%, run 2 vs. 97.3%, run 3) and o-chlorobenzene (93.4%, run 6 vs. 96.0%, run 7) hydrogenations. These results agree with previously reported studies on the role of Pt particle sizes in alumina-supported systems on their selectivity in of p-chloronitrobenzene hydrogenation [18].

The Pt/ $\gamma$ -Fe<sub>2</sub>O<sub>3</sub> system used in run 1 was magnetically recovered from the reaction mixture and reused till to 5 catalytic cycles showing no appreciable decline of its activity and selectivity (Fig. 3).

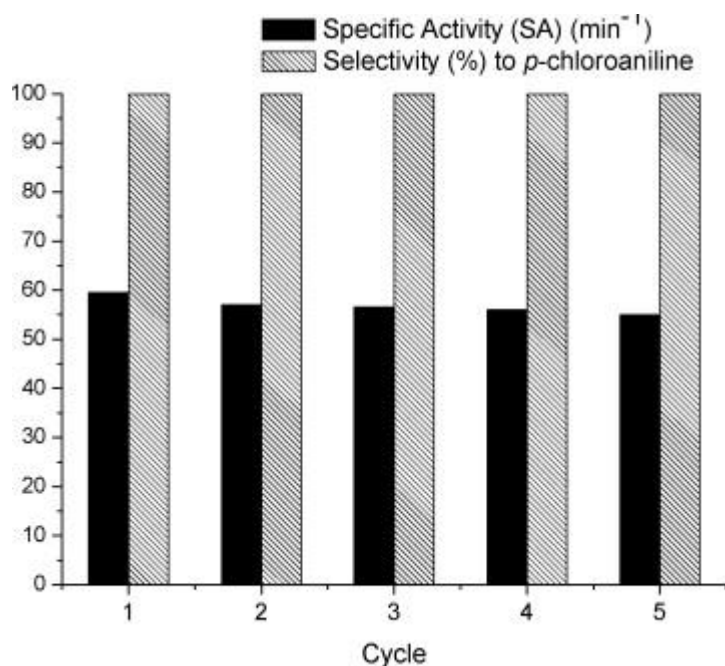


Fig. 3. Recycling tests of Pt/ $\gamma$ -Fe<sub>2</sub>O<sub>3</sub> catalysts.

XPS measurements of the Pt4f (Fig. 2, bottom), Fe2p and O1s core levels (Fig. 2, bottom) performed on the recovered Pt/ $\gamma$ -Fe<sub>2</sub>O<sub>3</sub> system after run 1 do not show appreciable BE shifts neither FWHM variation compared to the pristine sample (Fig. 2, top), as shown in Table 1, thus indicating that the chemical and electronic structure of the catalyst were not modified by the catalytic process.

Considering its good catalytic efficiency in the hydrogenation of *p*- and *o*-chloronitrobenzene, the Pt/ $\gamma$ -Fe<sub>2</sub>O<sub>3</sub> system was also tested in the hydrogenations of *m*-chloro-, bromo- and iodo-substituted nitrobenzenes (runs 8–11). The hydrogenation rates of *p*- and *o*-bromonitrobenzene (runs 8 and 9, respectively) over Pt/ $\gamma$ -Fe<sub>2</sub>O<sub>3</sub> system were higher than those of the corresponding chloro-derivatives while, with *p*- and *o*-iodonitrobenzene, a decrease in reaction rates occurred (runs 10 and 11, respectively).

The selectivity achieved towards the aniline derivatives were in any case very high (98.0–99.5%), that is higher than those of previously reported catalytic systems [33] and in agreement with the order of susceptibility to hydrogenolysis for aromatic halogens: Cl < Br < I; due to the increase of atomic number as well as electronegativity of halogen atom [34,35]. Finally, it is worth to note that, in any cases, extending of the reaction time after complete conversion of the halonitroaromatic substrate did not change the relative amount of the reaction products did not change and any decrease of haloaniline product was not observed.

#### 4. Conclusions

Mesitylene solvated Pt atoms, obtained by metal vapour synthesis and stabilized at 25 °C, provide a valuable precursor to prepare highly active supported platinum catalysts. TEM analysis confirms the efficiency of MVS method in the preparation of highly dispersed supported platinum catalysts containing metal nanoparticles with size controlled ranging 0.5–3.0 nm in diameter.

Therefore, in the catalytic hydrogenations of halonitroaromatics to the corresponding haloanilines, the support played a crucial role to control the catalytic efficiency rather than the metal particle size: indeed, the Pt/ $\gamma$ -Fe<sub>2</sub>O<sub>3</sub> system was significantly more active and selective than analogous  $\gamma$ -Al<sub>2</sub>O<sub>3</sub> supported system and a commercially available Pt/ $\gamma$ -Al<sub>2</sub>O<sub>3</sub> sample. Pt/ $\gamma$ -Fe<sub>2</sub>O<sub>3</sub> system exhibited considerable selectivity to haloaniline products under mild reaction conditions (25 °C, 0.1 MPa hydrogen pressure), leading to obtain *p*-chloroaniline as unique product in the hydrogenation of the corresponding *p*-chloronitrobenzene and very high selectivities ( $\geq 98\%$ ) with bromo- and iodobenzene derivatives.

XPS spectra of the Pt4f components on the Pt/ $\gamma$ -Fe<sub>2</sub>O<sub>3</sub> system indicate an electron polarization from Pt atoms to the  $\gamma$ -Fe<sub>2</sub>O<sub>3</sub> support. The resulting electron-deficient state of the Pt nanoparticles could improve the reactivity of the nitro group of the aromatic substrate taking into account the higher activity and selectivity of the Pt/ $\gamma$ -Fe<sub>2</sub>O<sub>3</sub> catalyst respect to the analogous sample supported on  $\gamma$ -Al<sub>2</sub>O<sub>3</sub>[34].

Moreover, the catalytic system can be magnetically recovered from the reaction mixture and used for at least five catalytic cycles without appreciable decline of its catalytic efficiency and, as evidenced by XPS analyses, without permanent modification of its chemical and/or electronic structure.

#### References

[1]

A.M. Tafesh, A.M. Weiguny

J. Chem. Rev., 96 (1996), pp. 2035-2052

[2]

N. Ono

The Nitro Group in Organic Synthesis

Wiley-VCH, New York (2001)

[3]

H.U. Blaser, U. Siegrist, H. Steiner, M. Studer

R.A. Sheldon, H. van Bekkum (Eds.), Fine Chemicals through Heterogeneous Catalysis, Wiley-VCH, Weinheim (2001), p. 389

[4]

V.L. Khilnani, B. Chandalia

Org. Process Dev., 5 (2001), pp. 257-262

[5]

X. Wang, M. Liang, J. Zhang, Y. Wang

Curr. Org. Chem., 11 (2007), pp. 299-314

[6]

R. Baltzy, A.P. Philips

J. Am. Chem. Soc., 68 (1946), pp. 261-265

[7]

F. Baralt, H. Holy

J. Org. Chem., 49 (1984), pp. 2626-2627

[8]

W.P. Dunworth, F.F. Nord

J. Am. Chem. Soc., 74 (1952), pp. 1459-1462

[9]

C.F. Winans

J. Am. Chem. Soc., 61 (1939), pp. 3564-3565

[10]

B.O. Pray, F.C. Trager, U.S. Patent 2,791,613 (1957).

[11]

A. Corma, C. Gonzalez-Arellano, M. Iglesias, F. Sanchez

Appl. Catal. A: Gen., 356 (2009), pp. 99-102

[12]

A. Corma, P. Serna

Science, 313 (2006), p. 332

[13]

R. Crook, J. Deering, S.J. Fussell, A.M. Happe, S. Mulvihill

Tetrahedron Lett., 51 (2010), pp. 5181-5184

[14]

P.N. Rylander

Catalytic Hydrogenations in Organic Syntheses

Academic Press, New York (1979)

[15]

G.G. Ferrier, F. King

Platinum Met. Rev., 27 (2) (1983), pp. 72-77

[16]

X. Han, R. Zhou, X. Zheng, H. Jiong

J. Mol. Catal. A: Chem., 193 (2003), pp. 103-108

ArticlePDF (100KB)

[17]

B. Coq, A. Tijani, F. Figueras

J. Mol. Catal., 68 (1991), pp. 331-345

[18]

B. Coq, A. Tijani, R. Dutartre, F. Figueras

J. Mol. Catal., 79 (1993), pp. 253-264

[19]

P. Serna, M. Boronat, A. Corma

Top. Catal., 54 (2011), p. 439

[20]

A. Corma, P. Serna, P. Concepcion, J.J. Calvino

J. Am. Chem. Soc., 130 (2008), pp. 1601-1610

[21]

J. Zhang, Y. Wang, H. Ji, Y. Wie, Y. Wu, B. Zuo, Q. Wang

J. Catal., 229 (2005), pp. 115-121

[22]

X. Wang, M. Liang, H. Liu, Y. Wang

J. Mol. Catal. A: Chem., 273 (2007), pp. 160-168

[23]

K.J. Klabunde

Free Atoms, Clusters and Nanoscale Particles

Academic Press, San Diego (1994)

[24]

G. Vitulli, C. Evangelisti, A.M. Caporusso, P. Pertici, N. Panziera, S. Bertozzi, P. Salvadori

B. Corain, G. Schmid, N. Toshima (Eds.), Metal Nanoclusters in Catalysis and Materials Science. The Issue of Size-control, Elsevier, Amsterdam (2008), pp. 437-451

[25]

G. Uccello-Barretta, C. Evangelisti, P. Raffa, F. Balzano, S. Nazzi, G. Martra, G. Vitulli, P. Salvadori

J. Organomet. Chem., 694 (2009), pp. 1813-1917

[26]

G. Vitulli, A. Verrazzani, E. Pitzalis, P. Salvadori, G. Capannelli, G. Martra

Catal. Lett., 44 (1997), pp. 205-210

[27]

P. Swift, D. Shuttleworth, M.P. Seah

D. Briggs, M.P. Seah (Eds.), Practical Surface Analysis by Auger and X-ray Photoelectron Spectroscopy, J. Wiley & Sons, Chichester (1983)

(Chapter 5, Appendix 3)

[28]

D.A. Shirley

Phys. Rev. B, 5 (12) (1972), pp. 4709-4714

[29]

I. Fratoddi, C. Battocchio, A. La Groia, M.V. Russo

J. Polym. Sci. A – Polym. Chem., 45 (15) (2007), pp. 3311-3329

[30]

I. Fratoddi, E.S. Bronze-Uhle, A. Batagin-Neto, D.M. Fernandes, E. Bodo, C. Battocchio, I. Venditti, F. Decker, M.V. Russo, G. Polzonetti, C.F.O. Graeff

J. Phys. Chem. A, 116 (34) (2012), pp. 8768-8774

[31]

NIST Standard Reference Database 20, Version 3.5, <http://srdata.nist.gov/xps/>.

[32]

G. Iucci, C. Battocchio, M. Dettin, R. Gambaretto, C. Di Bello, F. Borgatti, V. Carravetta, S. Monti, G. Polzonetti

Surf. Sci., 601 (18) (2007), pp. 3843-3849

[33]

M. Takasaki, Y. Motoyama, K. Higashi, S.-H. Yoon, I. Mochida, H. Nagashima

Org. Lett., 10 (2008), pp. 1601-1604

[34]

X. Wang, M. Liang, J. Zhang, Y. Wang

Curr. Org. Chem., 11 (2007), pp. 299-314

[35]

J.R. Kosak

W.H. Jones (Ed.), Catalysis in Organic Syntheses, Academic Press, New York (1980), p. 107